1003 – 7713/2001/05 – 0575 – 6

The Steady Shearing Flow Analysis of Polyaniline Type Electrorheological Fluids

Su Kai, Zhang Huizhen*, Li Xiucuo, Zhang Liucheng

(*Institute of Polymer Science and Engineering, Hebei University of Technology, Tianjin* 300130)

Abstract The yielding stresses or viscosity of electrorheological fluids increase by order of magnitude when electric fields are applied on them. The steady flow of electrorheological fluids based on polyaniline, polyaniline/(acrylic polyelectrolyte) composite particles were studied. The relationship between shear stress and shear rate under different AC field strengths was measured. Analysis is made to study the relationship between the yielding stress, as well as sensibility of shearing, and field strength. Furthermore, in the analysis under DC field strength, pseudoplastic behavior was found and interpreted. Distinctive differences of the flow behavior between the cases under DC and AC field were found. An original and effective expression was employed to characterize the flow behavior under a DC field.

Key words Electrorheological fluid, Shear stress, Shear rate, Polyaniline

1 Introduction

Electric fluid is the primary element of the creation of electrorheological effect. In earlier researches[1], we have developed a series of ERF based on polyaniline type electrorheological material. In this paper some key influences of field strength on steady shearing flow behavior are discussed to delve into manipulating conditions of the material. Some novel phenomena were found and interpreted.

2 Experiment details

Polyaniline was prepared by oxidization polymerization of aniline and using ammonium persulphate as oxidizer in the present of hydrochloric acid. The product particles were then filtered and washed by excess de-ionized water, and then collected. The material was further anti-doped by ammonia water whose pH value equals 10 for few hours. The result particles were then dried overnight under vacuum at 50℃. Anti-doped particles were sifted using a screen, whose mesh number is 300.

By emulsion polymerization the composite particles were synthesized as the procedure described below.

Certain amount of xylene and cetyl trimehyl ammonium bromide(CTAB) was added into a flask equipped with a reflux condenser, a stirrer, nitrogen protection and a thermometer. The system was then heated to 70℃ and well stirred for 30 min. Lithium acrylate (or acrylamide), anti-doped particles, ini-

* To whom correspondence should be addressed, Email: zhanghz2001@hotmail.com

Received date: 2001 – 08 – 14.

tiator(ammonium persulphate), and crosslinking agent(N,N'-methylene diacrylamide) were dissolved in certain amount of water and then added into the flask. The emulsion polymerization was kept under (65 ± 5)℃ for about 8 h. The result composite particles were then collected and dried under vacuum at 100℃ overnight.

Using different particles, the ERFs, with a volume concentration of 30%, were prepared employing silicone oil as dispersion media. The electrorheological effect was tested by a modified Rheotest II type concentric cylinder viscometer.

3 Results and discussion

The relationship of shear stress vs. shear rate and field strength under an electric load is very complicated. Early research[2] deems it conforms to Bingham model:

$$\tau = \tau_y(E) + \eta_a\dot{\gamma} \tag{1}$$

From this point of view, the relationship between shear stress and shear rate is linear. This phenomenon has been observed in some earlier studies[3,4].

Equation (1) consists of two parts: $\tau_y(E)$, which is a function of external field strength E, and $\eta_a\dot{\gamma}$, where η_a is a function of external field strength, shear deformation (γ) and shear rate($\dot{\gamma}$)[5]. So the overall influence of field strength on shear stress can be expressed as:

$$\tau = \tau_y(E) + \eta_a(E,\gamma,\dot{\gamma})\dot{\gamma} \tag{2}$$

In this paper the influence of E on yielding stress $\tau_y(E)$ is nominated on every figure by means of marking the intercept of every line, while the influence of E on η_a is indicated by the slope, which suggests the sensibility of shearing of the ERF, of each case.

3.1 Relationship between shear stress and shear rate under an AC field

We studied rheological behavior of different ERFs of PANI type under both DC and AC field load. Figures 13 show the behavior of ERFs under an alternative current.

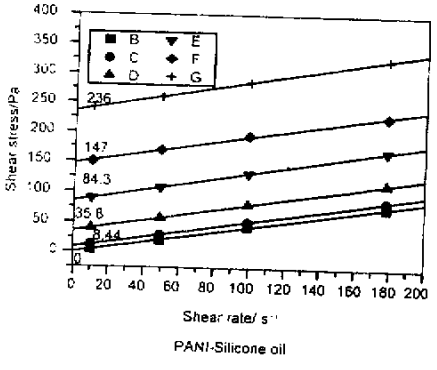

Fig. 1 Shear stress vs shear rate under different alternative field strength for PANI particles B: 0 kV, C: 1 kV, D: 2 kV, E: 3 kV, F: 4 kV, G: 5 kV/1.5 mm

The effect of shear rate on the shear stress at different field strength of ERFs based on anti – doped PANI was depicted in Fig. 1. The experiment results were fitted by linear regression analysis.

It is found in Fig. 1 that the data points can be considered to lie along straight line of a slight slope. This fact suggests that the ERFs essentially conform to Bingham behavior. By regression analysis of the result data, the slope, which indicates apparent viscosity η_a in equation (1), and intercept, which suggests yielding stress $\tau_y(E)$ there, were calculated. The relative low slope value (0.4-0.6) shows that the shearing sensibility of ERFs based on PANI particles is weak. Moreover, we also found that the slope value increases slightly with the promoting of field strength loaded. This reflects the sensibility of the ERFs become more pronounced as the field strength

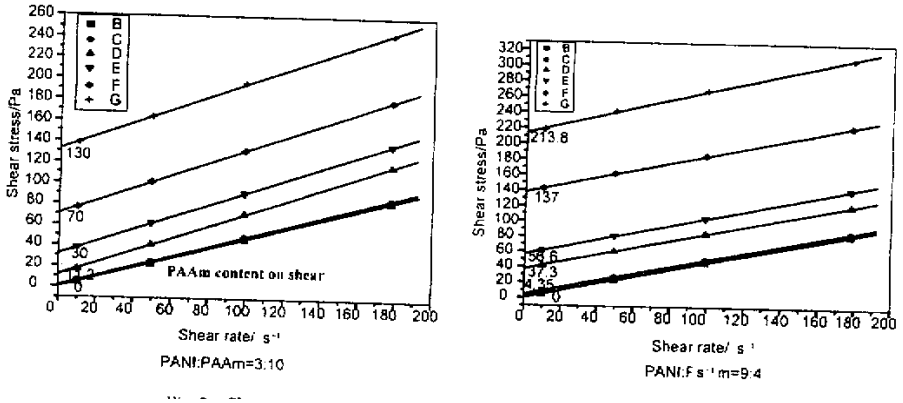

Fig.2 Shear stress vs shear rate under alternative field strength for PAAm
B∶0 kV, C∶1 kV, D∶2 kV, E∶3 kV, F∶4 kV, G∶5 kV/1.5 mm

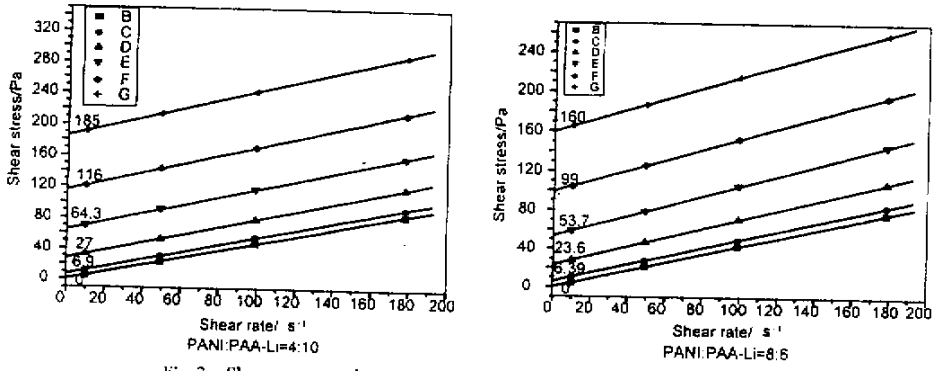

Fig.3 Shear stress vs shear rate under alternative field strength for PAA – Li
B∶0 kV, C∶1 kV, D∶2 kV, E∶3 kV, F∶4 kV, G∶5 kV/1.5 mm

increases.

These phenomena can be interpreted by the analysis of the internal structure changes of these ERFs under different filed strengths. Dispersed particles will aggregate along the direction of external field under the present of electric field. When the external field strength is relatively low, the aggregate structure of the dispersed particles is fragile, and the defects in the structure are relatively more. With the action of shearing force, the aggregate structure can be feasibly destroyed and it is not easy for the structure to recover. And with the raising of the external field strength, the aggregate structure becomes harder, and the defects are also less. Therefore the resistance to shearing force is great. So the apparent viscosity of the ERFs under high field strength is greater than that under relatively low field strength.

Another note – worthy feature of the curves in Fig.1 is the field – induced gap between the intercepts of each line. These gaps refer to the influence of external field strength E on τ_y. Some earlier literatures[5] have reported that the relationship between $\tau_y(E)$ and E conforms to the equation below,

$$\tau_y(E) = A E^n \tag{3}$$

From the information shown in Fig.1, these field – induced gaps increase with the increasing of external field strength. So, for the system we studied, the value of n is greater than unity.

Fig.23 show the steady flow behaviors of different ERFs based on polyaniline/poly (lithium acrylate) composite particles dispersed in silicone oil (hereafter expressed as PANI/PAA – Li – Silicone oil) and polyaniline/poly(acrylamide) composite particles dispersed in the same medium(hereafter expressed as PANI/PAAm – Silicone oil). From the results illustrated in Fig.23 above, it is indicated that the PANI/PAA – Li(or PAAm) – Silicone oil ERFs show very similar flow behavior as PANI ERFs .

With these comprehensive experiments, it may be concluded that, for the PANI type ERFs using silicone oil as the disperse medium: (i) the steady flow behavior approximately conforms to Bingham model and can be formulated as equation (2); (ii) the sensibility of the systems is relatively low and increase slightly with the field strength raising; (iii) the relationship between yielding strength and external field strength can be expressed as equation (3).

3.2 Relationship between shear stress and shear rate under an DC field

Generally, a Bingham model is used to present the behavior of relationship between shear stress and shear rate under both AC and DC field. Although this is approximately true, we found that the difference is so considerable that a new pseudoplastic model should be provided, as shown in Fig.47.

Cason introduced an useful model to characterize the flow behavior of pseudoplastic fluid. In this case, the relationship between shear stress and shear rate was formalized as the equation below:

$$\eta^{1/2}(E,\gamma,\dot{\gamma}) = \eta_{\infty}^{1/2} + \tau_y^{1/2}(E)\dot{\gamma}^{-1/2} \quad (4)$$

where $\eta_{\infty}(E)$ presents apparent viscosity under ultimate shearing. Transforming equation (4), a suitable function to characterize the flow behavior of ERFs we discussed is shown as equation (5).

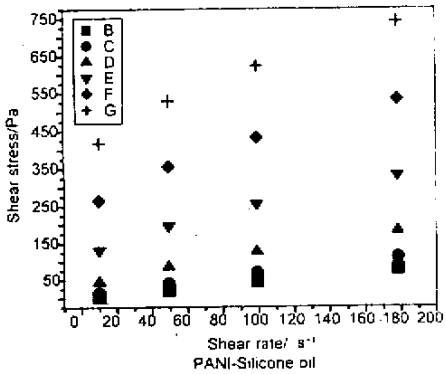

Fig.4 Shear stress vs shear rate under direct field strength for PANI
B: 0 kV; C: 1 kV; D: 2 kV; E: 3 kV; F: 4 kV; G: 5 kV/1.5 mm

$$\begin{cases} [\eta(E,\gamma,\dot{\gamma})\dot{\gamma}]^{1/2} = [\eta_{\infty}(E)\dot{\gamma}]^{1/2} + \tau_y^{1/2}(E) \\ [\eta(E,\gamma,\dot{\gamma})\dot{\gamma}]^{1/2} = \eta_{\infty}^{1/2}(E)\dot{\gamma}^{1/2} + \tau_y^{1/2}(E) \\ \tau^{1/2}(E,\gamma,\dot{\gamma}) = \eta_{\infty}^{1/2}(E)\dot{\gamma}^{1/2} + \tau_y^{1/2}(E) \end{cases} \quad (5)$$

Employing the equation we deduced, the data of Fig.4 were further processed. New result data were plotted in Fig.7. This time, shear stress square root and shear rate square root is used as Y and X axis respectively. The result points were fitted by the method of linear regression. It is obvious that the flow behavior of the ERFs we addressed conforms to the pseudoplastic model perfectly. By linear regression analysis, we found that $\eta_{\infty}(E)$ is essentially a constant. The calculating value is 0.44 (PANI). It should be noted that the other data shown in Fig.5, 6 are also processed and show an approximately similar result. From the analysis above, equation (5) can be used to simulate the flow behavior of some types of ERFs under DC field strength. Note that the equation consists of two individual parts. The first part $\eta_{\infty}^{1/2}(E)\dot{\gamma}^{1/2}$ relates to shear rate and external field strength, while the second part $\tau_y^{1/2}(E)$, which is the key element reflecting ER effect, relates to external field only.

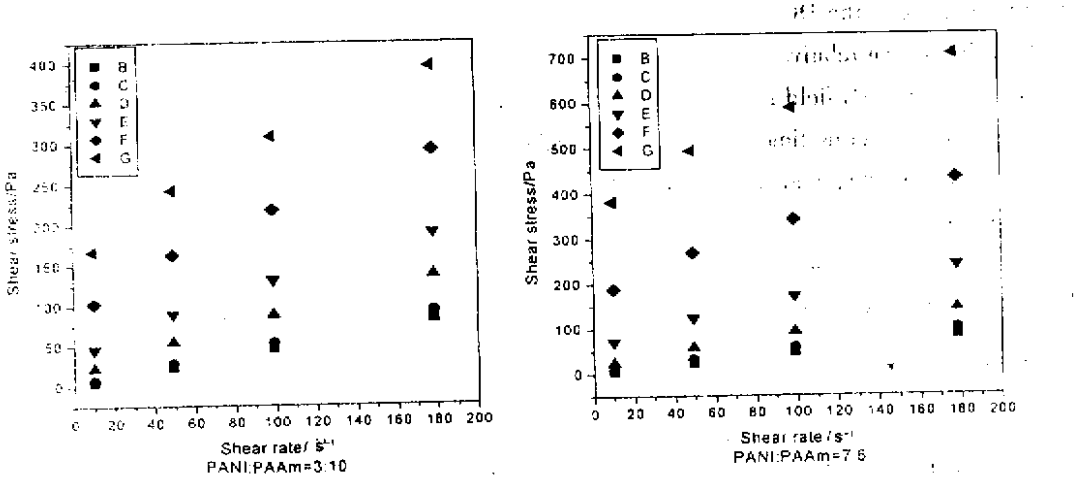

Fig.5 Shear stress vs shear rate under direct field strength for PAAm
B : 0 kV, C : 1 kV, D : 2 kV, E : 3 kV, F : 4 kV, G : 5 kV/1.5 mm

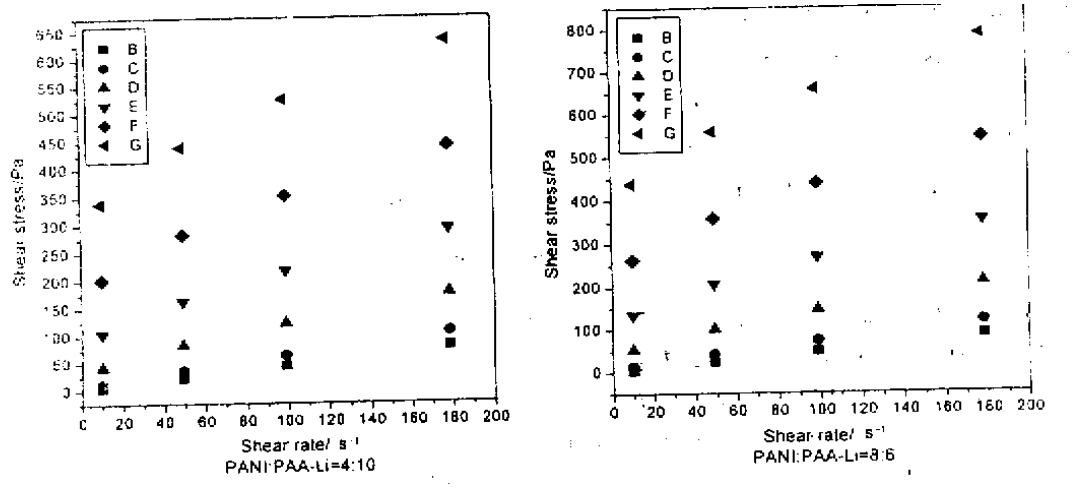

Fig.6 Shear stress vs shear rate under direct field strength for PAA – Li
B : 0 kV, C : 1 kV, D : 2 kV, E : 3 kV, F : 4 kV, G : 5 kV/1.5 mm

Different from the situation under an AC field, where the direction of the external field varies at a very frequency, the DC field keeps a changeless direction. This field condition makes the polarized particles form relatively steady aggregate structure in the suspension system, while the structures formed under an AC field keep on changing with the variation of direction of the external field. With the increasing of acting time of shearing, the relatively steady aggregate structures under the DC field become more fragile, and as a result, the resistance (or apparent viscosity) of the suspension to shearing reduces.

Since ERFs we concerned in this paper are relatively restricted in the ones based on poly (aniline) type, comprehensive studies are needed to delve into the flow behavior of ERFs.

4 Conclusions

1. By the method of linear regression, the experimental results were plotted. Under an AC field,

the ERFs exhibit a Bingham behavior shown below:

$$\tau = \tau_y(E) + \eta_a(E,\gamma,\dot{\gamma})\dot{\gamma}$$

2. Applying the same regression analysis, the flow behavior under a DC field is studied. Distinctive differences were observed in the same systems mentioned in (1). The steady shearing flow behavior in this case may conform to a pseudoplastic model shown below.

$$\tau^{1/2}(E,\gamma,\dot{\gamma}) = \tau_\infty^{1/2}(E)\dot{\gamma}^{1/2} + \tau_y^{1/2}(E)$$

3. The mechanisms of the phenomena observed in this paper were explained by the analysis of the field-induced aggregate structures of particles in the suspensions.

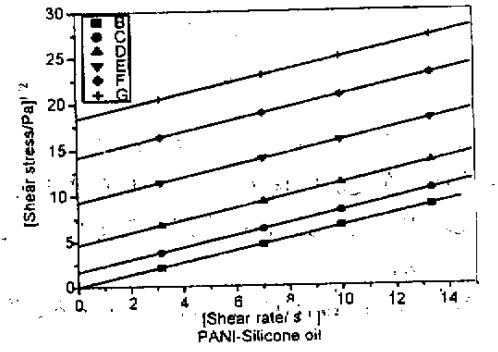

Fig.7 $\tau^{1/2}\dot{\gamma}^{1/2}$ curves corresponding to Fig.6

References

[1] Li X, Su K, Zhang L. *Mater. Rev.*, 2000, **5**: 70
[2] Uejima H. *J. Appl. Phys.*, 1972, **11**: 319
[3] Xu Y Z, *et al*.. *ERFs Proc. Int. Conf.*, 1992: 129
[4] Li X. Ph.D. Dissertation, Beijing Univ. Chem. Eng., 1997
[5] Sprecher A. F, *et al*.. *Mater. Sci. Eng.*, 1987, **95**: 187

聚苯胺类电流变体的稳态剪切流动分析

苏 恺, 张惠珍, 李秀错, 张留成

(河北工业大学高分子科学与工程研究所, 天津 300130)

摘 要: 对聚苯胺、及聚苯胺/聚丙烯酸盐复合粒子的稳态剪切流动行为进行了综合考察。结果表明, 在交流电场下, 电流变体的剪切应力和剪切速率的关系符合 Bingham 流体形为。并对此现象进行了分析, 提出用非理想塑性体的新模型来描述交流电场下聚苯胺类电流变体的稳态剪切流动。

关键词: 电流变液; 剪切应力; 剪切速率; 聚苯胺

* **通讯联系人**, Email: zhanghz2001@hotmail.com

收稿日期: 2001-08-14; **修回日期**: 2001-08-25。